

AttentionGAN: Unpaired Image-to-Image Translation using Attention-Guided Generative Adversarial Networks

Hao Tang, Hong Liu, Dan Xu, Philip H.S. Torr, Nicu Sebe

Abstract—State-of-the-art methods in the unpaired image-to-image translation are capable of learning a mapping from a source domain to a target domain with unpaired image data. Though the existing methods have achieved promising results, they still produce unsatisfied artifacts, being able to convert low-level information while limited in transforming high-level semantics of input images. One possible reason is that generators do not have the ability to perceive the most discriminative semantic parts between the source and target domains, thus making the generated images low quality. In this paper, we propose a new Attention-Guided Generative Adversarial Networks (AttentionGAN) for the unpaired image-to-image translation task. AttentionGAN can identify the most discriminative semantic objects and minimize changes of unwanted parts for semantic manipulation problems without using extra data and models. The attention-guided generators in AttentionGAN are able to produce attention masks via a built-in attention mechanism, and then fuse the generation output with the attention masks to obtain high-quality target images. Accordingly, we also design a novel attention-guided discriminator which only considers attended regions. Extensive experiments are conducted on several generative tasks, demonstrating that the proposed model is effective to generate sharper and more realistic images compared with existing competitive models. The source code of the proposed AttentionGAN is available at <https://github.com/Ha0Tang/AttentionGAN>.

Index Terms—Generative Adversarial Networks (GANs), Attention Mechanism, Unpaired Image-to-Image Translation

arXiv:1911.11897v3 [cs.CV] 28 Dec 2019

1 INTRODUCTION

Recently, Generative Adversarial Networks (GANs) [1] in various fields such as computer vision and image processing have produced powerful translation systems with supervised settings such as Pix2pix [2], where paired training images are required. However, the paired data are usually difficult and expensive to obtain. The input-output pairs for tasks such as artistic stylization could be even more difficult to acquire since the desired output is quite complex, typically requiring artistic authoring. To tackle this problem, CycleGAN [3], DualGAN [4] and DiscoGAN [5] provide a new insight, in which the GAN models can learn the mapping from a source domain to a target one with unpaired image data.

Despite these efforts, unpaired image-to-image translation, remains a challenging problem. Most existing models change unwanted parts in the translation, and can also be easily affected by background changes (see Fig. 1). In order to address these limitations, Liang et al. propose ContrastGAN [7], which uses object-mask annotations provided by the dataset to guide the generation. In ContrastGAN, it first crops the unwanted parts in the image based on the masks, and then pastes them back after the translation. While the

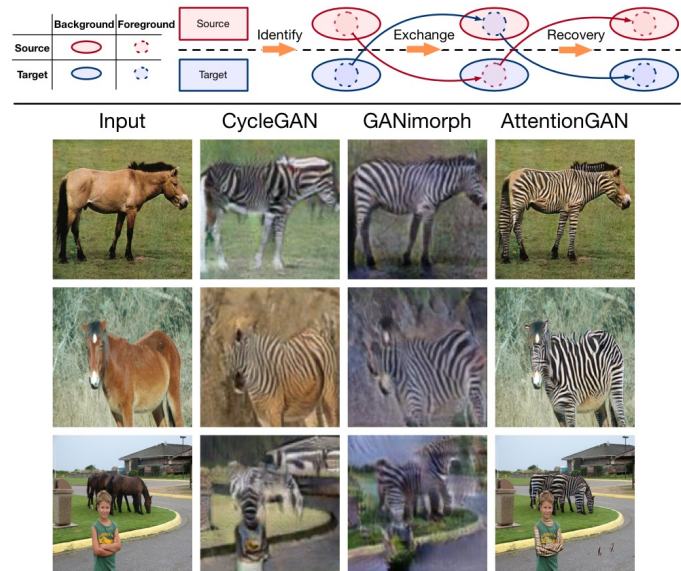


Fig. 1: The motivation of the proposed AttentionGAN (top) and a comparison with existing holistic image-to-image translation methods (e.g., CycleGAN [3] and GANimorph [6]) with an example of horse to zebra translation (bottom). Localizing the discriminative parts between the source domain and the target domain is a critical issue in the generation.

- Hao Tang and Nicu Sebe are with the Department of Information Engineering and Computer Science (DISI), University of Trento, Trento 38123, Italy. E-mail: hao.tang@unitn.it, sebe@disi.unitn.it.
- Hong Liu is with the Shenzhen Graduate School, Peking University, Shenzhen 518055, China. E-mail: hongliu@pku.edu.cn.
- Dan Xu and Philip H.S. Torr with the Department of Engineering Science, University of Oxford, Oxford OX1 2JD, United Kingdom. E-mail: danxu@robots.ox.ac.uk, phst@robots.ox.ac.uk.

Manuscript received April 19, 2015; revised August 26, 2015.

generated results are reasonable, it is hard to collect the training data with object-mask annotations. Another option is to train an extra model to detect the object masks and then employ them for the mask-guided generation [8], [9]. In this case, we need to significantly increase the network capacity,

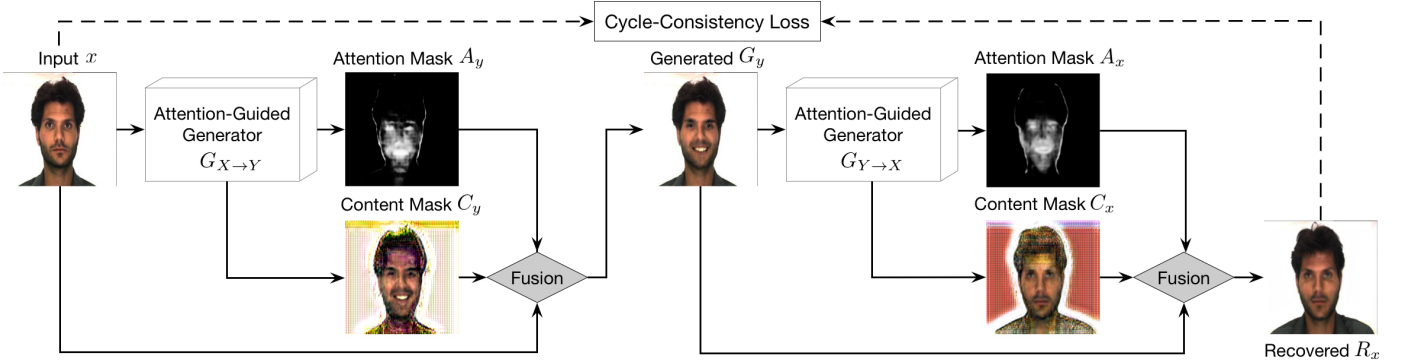


Fig. 2: The framework of the proposed attention-guided generation scheme I. We only show one mapping in this figure, i.e., $x \rightarrow [A_y, C_y] \rightarrow G_y \rightarrow [A_x, C_x] \rightarrow R_x \approx x$. We also have the other mapping, i.e., $y \rightarrow [A_x, C_x] \rightarrow G_x \rightarrow [A_y, C_y] \rightarrow R_y \approx y$. The attention-guided generators have a built-in attention module, which can perceive the most discriminative content between the source and target domains. We fuse the input image, the content mask and the attention mask to synthesize the targeted image.

which consequently raises the training complexity in both time and space.

To overcome the aforementioned issues, in this paper we propose a novel Attention-Guided Generative Adversarial Networks (AttentionGAN) for unpaired image translation task without using extra data and models. Fig. 1 illustrates the motivation of the proposed AttentionGAN and shows a comparison with existing holistic image translation methods using a horse to zebra translation example. The most important advantage of AttentionGAN is that the proposed generators can only focus on the foreground of the target domain and preserve the background of the source domain effectively. Specifically, the proposed generator learns both foreground and background attentions. It uses the foreground attention to select from the generated output for the foreground regions, while uses the background attention to maintain the background information from the input image. In this way, the proposed AttentionGAN can focus on the most discriminative foreground and ignore the unwanted background. We observe that the proposed AttentionGAN achieves significantly better results than both GANimorph [6] and CycleGAN [3]. As shown in Fig. 1, our AttentionGAN not only produces clearer results, but also successfully maintains the little boy in the background and only performs the translation for the horse behind it. However, the existing holistic image-to-image translation approaches are generally interfered by irrelevant background content, thus hallucinating texture patterns of the target objects.

We propose two different attention-guided generation schemes for the proposed AttentionGAN. The framework of the proposed scheme I is shown in Fig. 2. The proposed generator is equipped with a built-in attention module, which can disentangle the discriminative semantic objects from the unwanted parts via producing an attention mask and a content mask. Then we fuse the attention and the content masks to obtain the final generation. Moreover, we design a novel attention-guided discriminator which aims to consider only the attended foreground regions. The proposed attention-guided generator and discriminator are trained in an end-to-end fashion. The proposed attention-guided generation scheme I can achieve promising results on the facial expression translation as shown in Fig. 5,

where the change between the source and the target is relatively minor. However, it performs unsatisfactorily on more challenging scenarios in which more complex semantic translation is required, such as horse to zebra translation and apple to orange translation shown in Fig. 1. To tackle this issue, we further propose a more advanced attention-guided generation scheme, i.e. the scheme II, as depicted in Fig. 3. The improvement upon the scheme I is mainly three-fold: first, in the scheme I the attention mask and the content mask are generated with the same network. To have a more powerful generation of them, we employ two separate sub-networks in the scheme II; Second, in the scheme I we only generate the foreground mask to focus on the most discriminative semantic content. However, in order to better learn the foreground and preserve the background simultaneously, we produce both foreground and background attention masks in scheme II; Third, as the foreground generation is more complex, instead of learning a single content mask in the scheme I, we learn a set of several intermediate content masks, and correspondingly we also learn the same number of foreground attention masks. The generation of multiple intermediate content masks is beneficial for the network to learn a more rich generation space. The intermediate content masks are then fused with the foreground attention masks to produce the final content masks. Extensive experiments on several challenging public benchmarks demonstrate that the proposed scheme II can produce higher-quality target images compared with existing state-of-the-art methods.

The contribution of this paper is summarized as follows:

- We propose a new Attention-Guided Generative Adversarial Network (AttentionGAN) for unpaired image-to-image translation. This framework stabilizes the GANs training and thus improves the quality of generated images through jointly approximating attention and content masks with several losses and optimization methods.
- We design two novel attention-guided generation schemes for the proposed framework, in order to better perceive and generate the most discriminative foreground parts and simultaneously preserve well the unfocused objects and background. The proposed attention-guided generator and discriminator can be flexibly applied in other GAN models to improve the multi-domain image-

to-image translation, which we believe would also be beneficial to other related research.

- Extensive experiments are conducted on several publicly available datasets. The results show that the proposed AttentionGAN model can generate photo-realistic images with more clear details compared with existing state-of-the-art competitors. We also established new state-of-the-art results on these datasets.

The remainder of this paper is organized as follows. Sec. 2 introduces the related works of the image-to-image translation task. We then elaborate our AttentionGAN in Sec. 3, and in Sec. 4, we present the detailed experimental evaluation and discussion. Finally, we conclude the paper in Sec. 5.

2 RELATED WORK

Generative Adversarial Networks (GANs) [1] are powerful generative models, which have achieved impressive results on different computer vision tasks, e.g., image generation [10], [11]. In order to generate meaningful images that meet user requirements, Conditional GAN (CGAN) [12] employs the conditioned information to guide the image generation process. The conditioned information can be discrete labels [13], [14], object keypoints [15], human skeleton [16], semantic maps [17], [18] and reference images [2].

Paired Image-to-Image Translation models learn a translation function using CNNs. Pix2pix [2] is a conditional framework using a CGAN to learn a mapping function from input to output images. Wang et al. propose Pix2pixHD [17] for high-resolution photo-realistic image-to-image translation, which can be used for turning semantic label maps into photo-realistic images or synthesizing portraits from face label maps. Similar ideas have also been applied to many other tasks, such as hand gesture generation [16]. However, most of the tasks in the real world suffer from having few or none of the paired input-output samples available. When paired training data is not accessible, image-to-image translation becomes an ill-posed problem.

Unpaired Image-to-Image Translation. To overcome the aforementioned limitation, the unpaired image-to-image translation task has been proposed. In this task, the approaches learn the mapping function without the requirement of paired training data. Specifically, CycleGAN [3] learns the mappings between two image domains instead of the paired images. Apart from CycleGAN, many other GAN variants [4], [5], [14], [19], [20], [21], [22] are proposed to tackle the cross-domain problem. However, those models can be easily affected by unwanted content and cannot focus on the most discriminative semantic part of images during the translation stage.

Attention-Guided Image-to-Image Translation. To fix the aforementioned limitations, several works employ an attention mechanism to help image translation. Attention mechanisms have been successfully introduced in many applications in computer vision such as depth estimation [23], helping the models to focus on the relevant portion of the input to resolve the corresponding output without any supervision. In this spirit, several works use attention modules to attend to the region of interest for the image translation

task in an unsupervised way, which can be divided into two categories.

The first category is to use extra data to provide attention. For instance, Liang et al. propose ContrastGAN [7], which uses the object mask annotations from each dataset as extra input data. Sun et al. [24] generate a facial mask by using FCN for face attribute manipulation. Moreover, Mo et al. propose InstaGAN [25] that incorporates the instance information (e.g., object segmentation masks) and improves multi-instance transfiguration.

The second type is to train another segmentation or attention model to generate attention maps and fit it to the system. For example, Chen et al. [8] use an extra attention network to generate attention maps, so that more attention can be paid to objects of interests. Kastaniotis et al. present ATAGAN [9], which uses a teacher network to produce attention maps. Yang et al. [26] propose to add an attention module to predict an attention map to guide the image translation process. Zhang et al. propose SAGAN [27] for image generation task. Kim et al. [28] propose to use an auxiliary classifier to generate attention masks. Mejjati et al. [29] propose attention mechanisms that are jointly trained with the generators, discriminators and other two attention networks.

All these methods employ extra networks or data to obtain attention masks, which increases the number of parameters, training time and storage space of the whole system. Although these approaches performed an interesting exploration, we still observe unsatisfactory aspects mainly in the generated images. In this work, we propose a novel Attention-Guided Generative Adversarial Networks (AttentionGAN), which can produce attention masks by the generators. For this purpose, we embed an attention method to the vanilla generator meaning that we do not need any extra models to obtain the attention masks of objects of interests. AttentionGAN learns to attend to key parts of the image while keeping everything else unaltered, essentially avoiding undesired artifacts or changes. Most importantly, the proposed methods can be applied to any GAN-based framework for unpaired [3], paired [2] and multi-domain [14] image-to-image translation tasks.

3 ATTENTION-GUIDED GENERATIVE ADVERSARIAL NETWORKS

We first start with the attention-guided generator and discriminator of the proposed AttentionGAN, and then introduce the loss function for better optimization of the model. Finally, we present the implementation details of the whole model including network architecture and training procedure.

3.1 Attention-Guided Generator

Background. GANs [1] are composed of two competing modules, i.e., the generator $G_{X \rightarrow Y}$ and the discriminator D_Y (where X and Y denote two different image domains), which are iteratively trained competing against with each other in the manner of two-player mini-max. More formally, let $x_i \in X$ and $y_j \in Y$ denote the training images in source and target image domain, respectively (for simplicity, we usually

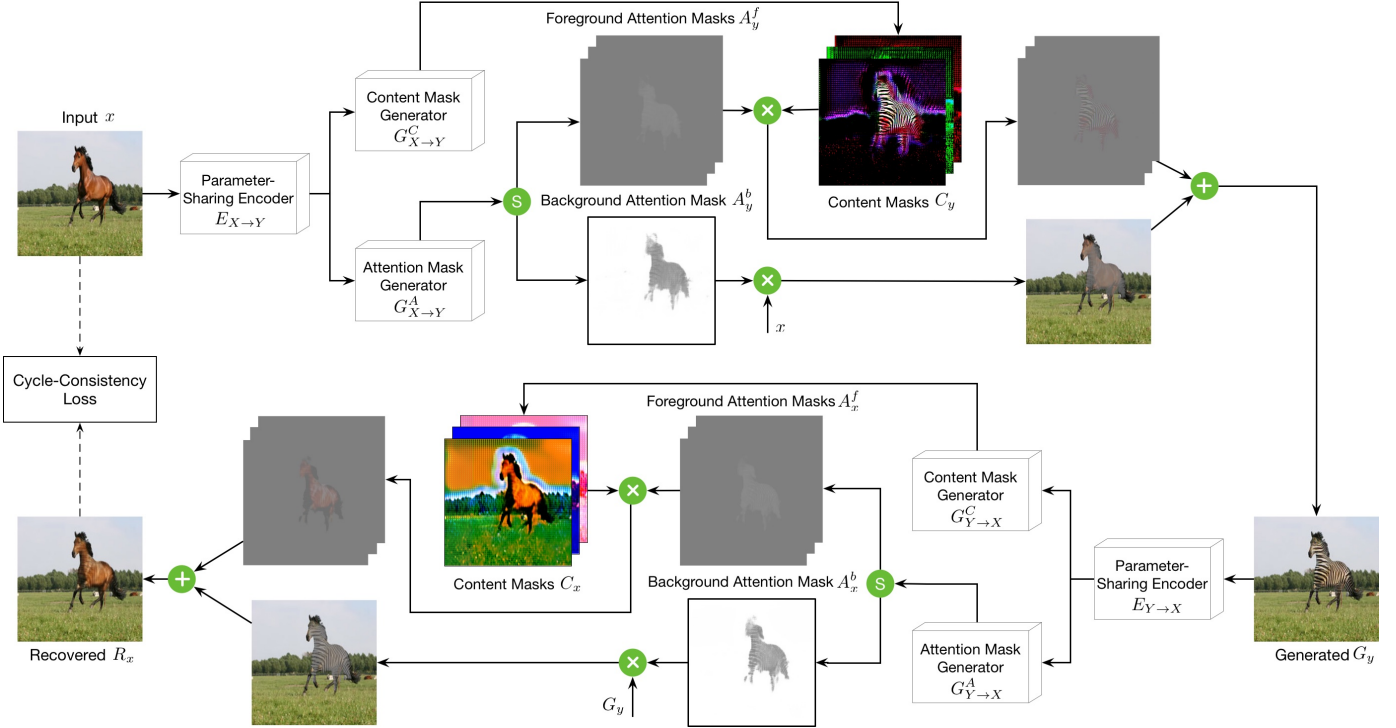


Fig. 3: The framework of the proposed attention-guided generation scheme II. We only show one mapping in this figure, i.e., $x \rightarrow G_y \rightarrow R_x \approx x$. We also have the other mapping, i.e., $y \rightarrow G_x \rightarrow R_y \approx y$. Each generator such as $G_{X \rightarrow Y}$ consists of a parameter-sharing encoder $E_{X \rightarrow Y}$, an attention mask generator $G_{X \rightarrow Y}^A$ and a content mask generator $G_{X \rightarrow Y}^C$. $G_{X \rightarrow Y}^A$ aims to produce attention masks of both foreground and background to attentively select the useful content from the corresponding content masks generated by $G_{X \rightarrow Y}^C$. The proposed model is constrained by the cycle-consistency loss and trained in an end-to-end fashion. The symbols \oplus , \otimes and \textcircled{S} denote element-wise addition, element-wise multiplication and channel-wise Softmax, respectively.

omit the subscript i and j). For most current image translation models, e.g., CycleGAN [3] and DualGAN [4], they include two mappings $G_{X \rightarrow Y}: x \rightarrow G_y$ and $G_{Y \rightarrow X}: y \rightarrow G_x$, and two corresponding adversarial discriminators D_X and D_Y . Generator $G_{X \rightarrow Y}$ maps x from the source domain to the generated image G_y in the target domain Y and tries to fool the discriminator D_Y , whilst D_Y focuses on improving itself in order to be able to tell whether a sample is a generated sample or a real data sample. Similar to $G_{Y \rightarrow X}$ and D_X .

Attention-Guided Generation Scheme I. For the proposed AttentionGAN, we intend to learn two mappings between domains X and Y via two generators with built-in attention mechanism, i.e., $G_{X \rightarrow Y}: x \rightarrow [A_y, C_y] \rightarrow G_y$ and $G_{Y \rightarrow X}: y \rightarrow [A_x, C_x] \rightarrow G_x$, where A_x and A_y are the attention masks of images x and y , respectively; C_x and C_y are the content masks of images x and y , respectively; G_x and G_y are the generated images. The attention masks A_x and A_y define a per pixel intensity specifying to which extent each pixel of the content masks C_x and C_y will contribute in the final rendered image. In this way, the generator does not need to render static elements, and can focus exclusively on the pixels defining the domain content movements, leading to sharper and more realistic synthetic images. After that, we fuse input image x and the generated attention mask A_y , and the content mask C_y to obtain the targeted image G_y . In this way, we can disentangle the most discriminative semantic object and unwanted part of images. Take Fig. 2 for example, the attention-guided generators focus only on

those regions of the image that are responsible of generating the novel expression such as eyes and mouth, and keep the rest of parts of the image such as hair, glasses, clothes untouched. The higher intensity in the attention mask means the larger contribution for changing the expression.

The input of each generator is a three-channel image, and the outputs of each generator are an attention mask and a content mask. Specifically, the input image of $G_{X \rightarrow Y}$ is $x \in \mathbb{R}^{H \times W \times 3}$, and the outputs are the attention mask $A_y \in \{0, \dots, 1\}^{H \times W}$ and content mask $C_y \in \mathbb{R}^{H \times W \times 3}$. Thus, we use the following formula to calculate the final image G_y ,

$$G_y = C_y * A_y + x * (1 - A_y), \quad (1)$$

where the attention mask A_y is copied to the three channels for multiplication purpose. Intuitively, the attention mask A_y enables some specific areas where domain changed to get more focus and applying it to the content mask C_y can generate images with clear dynamic area and unclear static area. The static area should be similar between the generated image and the original real image. Thus, we can enhance the static area (basically it refers to background area) in the original real image $(1 - A_y) * x$ and merge it to $C_y * A_y$ to obtain final result $C_y * A_y + x * (1 - A_y)$. The formulation for generator $G_{Y \rightarrow X}$ and input image y can be expressed as $G_x = C_x * A_x + y * (1 - A_x)$.

Limitations. The proposed attention-guided generation scheme I performs well on the tasks where the source domain and the target domain have large overlap similarity

such as the facial expression-to-expression translation task. However, we observe that it cannot generate photo-realistic images on complex tasks such as horse to zebra translation, as shown in Fig. 5. The drawbacks of the scheme I are three-fold: (i) The attention and the content mask are generated by the same network, which could degrade the quality of the generated images; (ii) We observe that the scheme I only produces one attention mask to simultaneously change the foreground and preserve the background of the input images; (iii) We observe that scheme I only produces one content mask to select useful content for generating the foreground content, which means the model does not have enough ability to deal with complex tasks such as horse to zebra translation. To solve these limitations, we further propose a more advanced attention-guided generation scheme II as shown in Fig. 3.

Attention-Guided Generation Scheme II. Scheme I adopts the same network to produce both attention and content masks and we argue that this will degrade the generation performance. In scheme II, the proposed generators $G_{X \rightarrow Y}$ and $G_{Y \rightarrow X}$ are composed of two sub-nets each for generating attention masks and content masks as shown in Fig. 3. For instance, $G_{X \rightarrow Y}$ is comprised of a parameter-sharing encoder $E_{X \rightarrow Y}$, an attention mask generator $G_{X \rightarrow Y}^A$ and a content mask generator $G_{X \rightarrow Y}^C$. $E_{X \rightarrow Y}$ aims at extracting both low-level and high-level deep feature representations. $G_{X \rightarrow Y}^C$ targets to produce multiple intermediate content masks. $G_{X \rightarrow Y}^A$ tries to generate multiple attention masks. In the way, both attention mask generation and content mask generation have their own network parameters and will not interfere with each other.

To fix the limitation (ii) of the scheme I, in scheme II the attention mask generator $G_{X \rightarrow Y}^A$ targets to generate both $n-1$ foreground attention masks $\sum_1^{n-1} A_y^f$ and one background attention mask A_y^b . By doing so, the proposed network can simultaneously learn the novel foreground and preserve the background of input images. The key point success of the proposed scheme II in unpaired image-to-image translation problems are foreground and background attention masks, which allow the model to modify the foreground and simultaneously preserve the background of input images, and this is exactly the goal that unpaired image-to-image translation tasks aim to optimize.

Moreover, we observe that in some generation tasks such as horse to zebra translation, the foreground generation is very difficult if we only produce one content mask as did in scheme I. To solve this limitation, we use the content mask generator $G_{X \rightarrow Y}^C$ to produce $n-1$ content masks, i.e., $\sum_1^{n-1} C_y$. Then with the input image x , we obtain n intermediate content masks. In this way, a 3-channel generation space can be enlarged to a $3*n$ -channel generation space, which is suitable for learning a good mapping for complex image-to-image translation.

Finally, the attention masks are multiplied by the corresponding content masks to obtain the final target result. Formally, this is written as:

$$G_y = \sum_1^{n-1} (C_y * A_y^f) + x * A_y^b, \quad (2)$$

where n attention masks $[\sum_1^{n-1} A_y^f, A_y^b]$ are produced by

a channel-wise softmax activation function for the normalization. In this way, we can preserve the background of the input image x , i.e., $x * A_y^b$, and simultaneously generate the novel foreground content for the input image, i.e., $\sum_1^{n-1} (C_y * A_y^f)$. Next, we merge the generated foreground $\sum_1^{n-1} (C_y * A_y^f)$ to the background of the input image $x * A_y^b$ to obtain the final result G_y .

Attention-Guided Generation Cycle. To further regularize the mappings, we adopt two cycles in our AttentionGAN as shown in Fig. 3. The cycle-consistency has been shown to be very useful in unpaired image-to-image translation task [3]. The motivation of the cycle-consistency is that if we translate from one domain to the other and back again we should arrive at where we started. More specifically, after generating the result G_y by $G_{X \rightarrow Y}$, we should push back G_y to the original domain. Thus we introduce another generator $G_{Y \rightarrow X}$, which has a similar structure to the generator $G_{X \rightarrow Y}$ and also consists of three sub-nets, i.e., a parameter-sharing encoder $E_{Y \rightarrow X}$, an attention mask generator $G_{Y \rightarrow X}^A$ and a content mask generator $G_{Y \rightarrow X}^C$. $G_{Y \rightarrow X}^C$ tries to generate $n-1$ content masks (i.e., $\sum_1^{n-1} C_x$) and $G_{Y \rightarrow X}^A$ tries to generate n attention masks of both background and foreground (i.e., A_x^b and $\sum_1^{n-1} A_x^f$). Then we fuse both masks and the generated image G_y to reconstruct the original input image x and this process can be formulated as,

$$R_x = \sum_1^{n-1} (C_x * A_x^f) + G_y * A_x^b. \quad (3)$$

For better learning both cycles, we further adopt the cycle-consistency loss to reduce the space of possible mapping, this loss can be formulated as,

$$\mathcal{L}_{cycle}(G_{X \rightarrow Y}, G_{Y \rightarrow X}) = \mathbb{E}_{x \sim p_{data}(x)} [\|R_x - x\|_1] + \mathbb{E}_{y \sim p_{data}(y)} [\|R_y - y\|_1], \quad (4)$$

where the reconstructed images $R_x = G_{Y \rightarrow X}(G_{X \rightarrow Y}(x))$ is closely matched to the input image x , and is similar to the generated image $R_y = G_{X \rightarrow Y}(G_{Y \rightarrow X}(y))$ and the input image y . This could lead to generators to further reduce the space of possible mappings.

3.2 Attention-Guided Discriminator

Eq. (1) constrains the generators to act only on the attended regions. However, the discriminators currently consider the whole image. More specifically, the vanilla discriminator D_Y takes the generated image G_y or the real image y as input and tries to distinguish them. This is similar to the discriminator D_X , which tries to distinguish between the generated image G_x and the real image x . To add an attention mechanism to the discriminator, we propose two attention-guided discriminators. The attention-guided discriminator is structurally the same as the vanilla discriminator but it also takes the attention mask as input. The attention-guided discriminator D_{YA} tries to distinguish between the fake image pairs $[A_y, G_y]$ and the real image pairs $[A_y, y]$. This is similar to D_{XA} , which tries to distinguish the fake image pairs $[A_x, G_x]$ and the real image pairs $[A_x, x]$. In this way, the discriminators can focus on the most discriminative content and ignore the unrelated content.

3.3 Optimization Objective

Adversarial Loss. We apply an adversarial loss [1] to optimize the proposed AttentionGAN. For the mapping $G_{X \rightarrow Y}: x \rightarrow G_y$ and its discriminator D_Y , the loss can be formulated as follows:

$$\mathcal{L}_{GAN}(G_{X \rightarrow Y}, D_Y) = \mathbb{E}_{y \sim p_{\text{data}}(y)} [\log D_Y(y)] + \mathbb{E}_{x \sim p_{\text{data}}(x)} [\log(1 - D_Y(G_{X \rightarrow Y}(x)))] \quad (5)$$

$G_{X \rightarrow Y}$ tries to minimize the adversarial loss objective $\mathcal{L}_{GAN}(G_{X \rightarrow Y}, D_Y)$ while D_Y tries to maximize it. The target of $G_{X \rightarrow Y}$ is to generate an image $G_y = G_{X \rightarrow Y}(x)$ that looks similar to the images from domain Y , while D_Y aims to distinguish between the generated images $G_{X \rightarrow Y}(x)$ and the real images y . A similar adversarial loss of Eq. (5) for mapping $G_{Y \rightarrow X}$ and its discriminator D_X is defined as $\mathcal{L}_{GAN}(G_{Y \rightarrow X}, D_X) = \mathbb{E}_{x \sim p_{\text{data}}(x)} [\log D_X(x)] + \mathbb{E}_{y \sim p_{\text{data}}(y)} [\log(1 - D_X(G_{Y \rightarrow X}(y)))]$.

Attention-Guided Adversarial Loss. We propose the attention-guided adversarial loss for training the attention-guide discriminators. The min-max game between the attention-guided discriminator D_{YA} and the generator $G_{X \rightarrow Y}$ is performed through the following objective functions:

$$\mathcal{L}_{AGAN}(G_{X \rightarrow Y}, D_{YA}) = \mathbb{E}_{y \sim p_{\text{data}}(y)} [\log D_{YA}([A_y, y])] + \mathbb{E}_{x \sim p_{\text{data}}(x)} [\log(1 - D_{YA}([A_y, G_{X \rightarrow Y}(x)]))] \quad (6)$$

where D_{YA} aims to distinguish between the generated image pairs $[A_y, G_{X \rightarrow Y}(x)]$ and the real image pairs $[A_y, y]$. We also have another loss $\mathcal{L}_{AGAN}(G_{Y \rightarrow X}, D_{XA})$ for discriminator D_{XA} and the generator $G_{Y \rightarrow X}$.

Attention Loss. When training our AttentionGAN we do not have ground-truth annotation for the attention masks. They are learned from the resulting gradients of both attention-guided generators and discriminators and the rest of the losses. However, the attention masks can easily saturate to 1 causing the attention-guided generators to have no effect as indicated in GANimation [30]. To prevent this situation, we perform a Total Variation regularization over attention masks A_x and A_y . The attention loss of mask A_x therefore can be defined as:

$$\mathcal{L}_{tv}(M_x) = \sum_{w, h=1}^{W, H} |A_x(w+1, h, c) - A_x(w, h, c)| + |A_x(w, h+1, c) - A_x(w, h, c)| \quad (7)$$

where W and H are the width and height of A_x .

Pixel Loss. To reduce changes and constrain the generator in scheme I, we adopt pixel loss between the input images and the generated images. We express this loss as:

$$\mathcal{L}_{pixel}(G_{X \rightarrow Y}, G_{Y \rightarrow X}) = \mathbb{E}_{x \sim p_{\text{data}}(x)} [\|G_{X \rightarrow Y}(x) - x\|_1] + \mathbb{E}_{y \sim p_{\text{data}}(y)} [\|G_{Y \rightarrow X}(y) - y\|_1] \quad (8)$$

We adopt $L1$ distance as loss measurement in pixel loss. Note that the pixel loss has been usually used in the paired image translation models such as Pix2pix [2]. However, we use this loss for the unpaired image translation task.

Full Objective. The complete objective loss of the proposed AttentionGAN can be formulated as follows:

$$\mathcal{L} = [\lambda_{cycle} * \mathcal{L}_{cycle} + \lambda_{pixel} * \mathcal{L}_{pixel}] * r + [\lambda_{gan} * (\mathcal{L}_{GAN} + \mathcal{L}_{AGAN}) + \lambda_{tv} * \mathcal{L}_{tv}] * (1 - r), \quad (9)$$

where λ_{gan} , λ_{cycle} , λ_{pixel} and λ_{tv} are parameters controlling the relative relation of objectives terms; r is a curriculum parameter to control the relation between GAN loss and reconstruction loss (i.e, cycle-consistency loss and pixel loss) during curriculum period. We also adopt the identity preserving loss $\lambda_{id} \mathcal{L}_{id}$ proposed in CycleGAN to encourage the mapping to preserve the identity information such as color.

3.4 Implementation Details

Network Architecture. For a fair comparison, we use the generator architecture from CycleGAN [3]. We have slightly modified it for our task. Scheme I takes a three-channel RGB image as input and outputs a single-channel attention mask and a three-channel content mask. Scheme II takes a three-channel RGB image as input and outputs n attention masks and $n-1$ content masks, thus we fuse all of these masks and the input image to produce the final results. We set $n=10$ in our experiments. For the vanilla discriminator, we employ the discriminator architecture from [2], [3]. We employ the same architecture as the proposed attention-guided discriminator except the attention-guided discriminator takes a attention mask and an image as inputs while the vanilla discriminator only takes an image as input.

Training Strategy. We follow the standard optimization method from [1] to optimize the proposed AttentionGAN, i.e., we alternate between one gradient descent step on generators, then one step on discriminators. Moreover, to slow down the rate of discriminators relative to generators we follow CycleGAN [3] and divide the objective by 2 while optimizing discriminators. We use a least square loss [31] to stabilize our model during the training procedure similar to CycleGAN. We also use a history of generated images to update discriminators similar to CycleGAN.

4 EXPERIMENTS

To explore the generality of the proposed AttentionGAN, we evaluate the proposed model on a variety of tasks with both face and natural images, including facial expression translation, facial attribute transfer, horse \leftrightarrow zebra translation, apple \leftrightarrow orange translation, map \leftrightarrow aerial photo translation and style transfer. The proposed AttentionGAN is implemented using public PyTorch framework. The source code and trained models are available at <https://github.com/Ha0Tang/AttentionGAN>.

4.1 Experimental Setup

Datasets. We employ eight publicly available datasets to evaluate the proposed AttentionGAN, including four face image datasets (i.e., CelebA, RaFD, AR Face and Selfie2anime) and four natural image datasets. (i) CelebA dataset [32] has more than 200K celebrity images with complex backgrounds, each annotated with about 40 attributes. We use this dataset for multi-domain facial attribute transfer task. Following StarGAN [14], we select 2,000 images for testing and use all remaining images for training. Seven

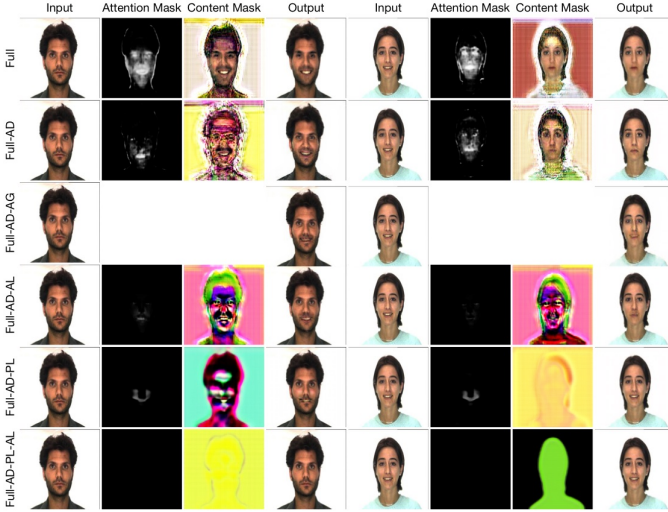


Fig. 4: Ablation study of the proposed AttentionGAN.

TABLE 1: Ablation study of the proposed AttentionGAN.

Setup of AttentionGAN	AMT \uparrow	PSNR \uparrow
Full	12.8	14.9187
Full - AD	10.2	14.6352
Full - AD - AG	3.2	14.4646
Full - AD - PL	8.9	14.5128
Full - AD - AL	6.3	14.6129
Full - AD - PL - AL	5.2	14.3287

facial attributes, i.e. gender (male/female), age (young/old), hair color (black, blond, brown) are adopted in our experiments. Moreover, in order to evaluate the performance of the proposed AttentionGAN under the situation where training data is limited. We conduct facial expression translation experiments on this dataset. Specifically, we randomly select 1,000 neutral images and 1,000 smile images as training data, and another 1,000 neutral and 1,000 smile images as testing data. (ii) RaFD dataset [33] consists of 4,824 images collected from 67 participants. Each participant have eight facial expressions. We employ all of the images for multi-domain facial expression translation task. (iii) AR Face [34] contains over 4,000 color images in which only 1,018 images have four different facial expressions, i.e., smile, anger, fear and neutral. We employ the images with the expression labels of smile and neutral to evaluate our method. (iv) We follow U-GAT-IT [28] and use the Selfie2anime dataset to evaluate the proposed AttentionGAN. (v) Horse and zebra dataset [3] has been downloaded from ImageNet using keywords wild horse and zebra. The training set size of horse and zebra are 1067 (horse) and 1334 (zebra). The testing set size of horse and zebra are 120 (horse) and 140 (zebra). (vi) Apple and orange dataset [3] is also collected from ImageNet using keywords apple and navel orange. The training set size of apple and orange are 996 (apple) and 1020 (orange). The testing set size of apple and orange are 266 (apple) and 248 (orange). (vii) Map and aerial photograph dataset [3] contains 1,096 training and 1,098 testing images for both domains. (viii) We use the style transfer dataset proposed in [3]. The training set size of each domain is 6,853 (Photo), 1074 (Monet), 584 (Cezanne).

Parameter Setting. For all datasets, images are re-scaled to 256×256 . We do left-right flip and random crop for data augmentation. We set the number of image buffer to 50 similar in [3]. We use the Adam optimizer [35] with the

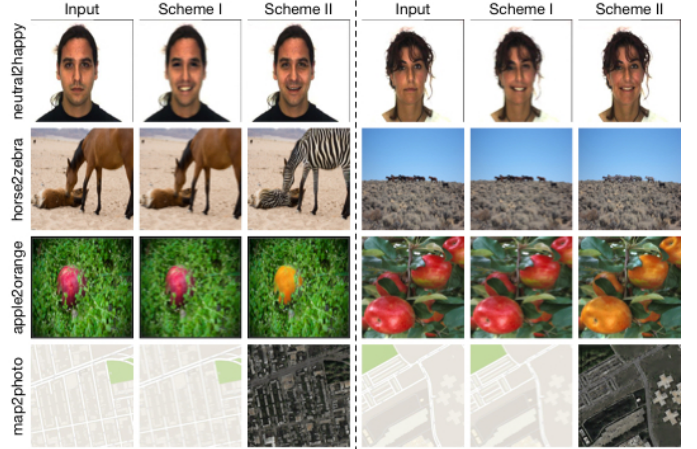


Fig. 5: Comparison results of the proposed attention-guided generation scheme I and II.

momentum terms $\beta_1=0.5$ and $\beta_2=0.999$. For experiments on face datasets, we follow [36] and set $\lambda_{cycle}=10$, $\lambda_{gan}=0.5$, $\lambda_{pixel}=1$ and $\lambda_{tv}=1e-6$. For r in Eq. (9), we set it to 0.01 at the first 10 epochs. After curriculum period, we set r to 0.5. For experiments on natural image datasets, we follow CycleGAN [3] and set $\lambda_{cycle}=10$, $\lambda_{id}=0.5$.

Competing Models. We consider several state-of-the-art image translation models as our baselines. (i) Unpaired image translation methods: CycleGAN [3], DualGAN [4], DIAT [37], DiscoGAN [5], DistanceGAN [19], Dist.+Cycle [19], Self Dist. [19], ComboGAN [20], UNIT [38], MUNIT [39], DRIT [40], GANimorph [6], CoGAN [41], SimGAN [42], Feature loss+GAN [42] (a variant of SimGAN); (ii) Paired image translation methods: BicycleGAN [43], Pix2pix [2], Encoder-Decoder [2]; (iii) Class label, object mask or attention-guided image translation methods: IcGAN [13], StarGAN [14], ContrastGAN [7], GANimation [30], RA [44], UAIT [29], U-GAT-IT [28], SAT [26]; (iv) Unconditional GANs methods: BiGAN/ALI [45], [46]. Note that the fully supervised Pix2pix, Encoder-Decoder (Enc-Decoder) and BicycleGAN are trained with paired data. Since BicycleGAN can generate several different outputs with one single input image, we randomly select one output from them for fair comparisons. To re-implement ContrastGAN, we use OpenFace [47] to obtain the face masks as extra input data.

Evaluation Metrics. Following CycleGAN [3], we adopt Amazon Mechanical Turk (AMT) perceptual studies to evaluate the generated images. We gather data from 50 participants per algorithm we tested. Participants were shown a sequence of pairs of images, one real image and one fake (generated by our method or a baseline), and asked to click on the image they thought was real. To seek a quantitative measure that does not require human participation, Peak Signal-to-Noise Ratio (PSNR), Kernel Inception Distance (KID) [48] and Fréchet Inception Distance (FID) [49] are employed according to different translation tasks.

4.2 Experimental Results

4.2.1 Ablation Study

Analysis of Model Component. To evaluate the components of our AttentionGAN, we first conduct extensive

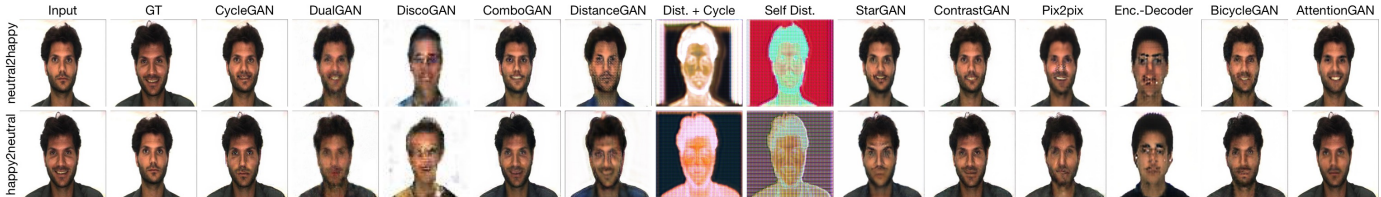


Fig. 6: Comparison with different methods on AR Face datasets.

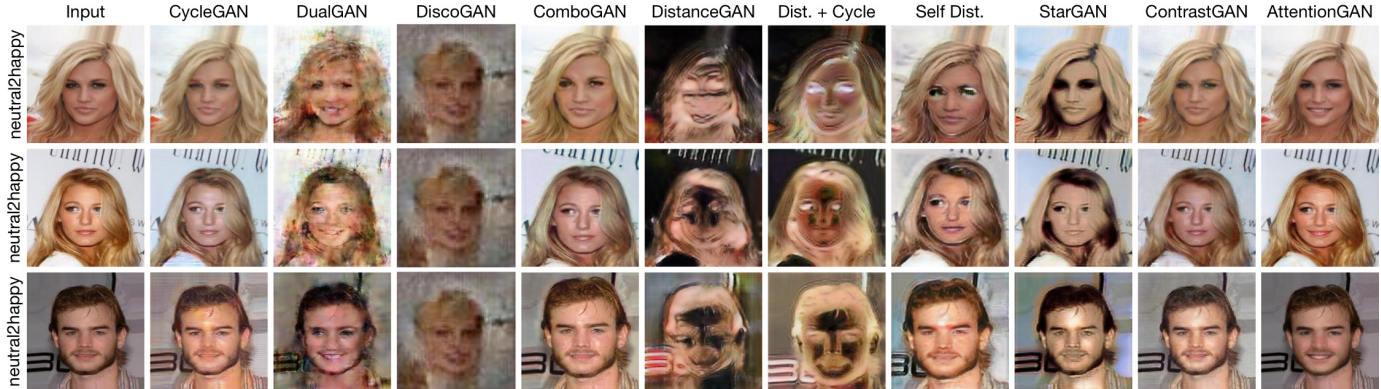


Fig. 7: Comparison with different methods on CelebA dataset for facial expression transfer task.

TABLE 2: Quantitative comparison with different models on facial expression translation task. For both AMT and PSNR, high is better.

Model	Publish	AR Face		CelebA
		AMT \uparrow	PSNR \uparrow	AMT \uparrow
CycleGAN [3]	ICCV 2017	10.2	14.8142	34.6
DualGAN [4]	ICCV 2017	1.3	14.7458	3.2
DiscoGAN [5]	ICML 2017	0.1	13.1547	1.2
ComboGAN [20]	CVPR 2018	1.5	14.7465	9.6
DistanceGAN [19]	NIPS 2017	0.3	11.4983	1.9
Dist.+Cycle [19]	NIPS 2017	0.1	3.8632	1.3
Self Dist. [19]	NIPS 2017	0.1	3.8674	1.2
StarGAN [14]	CVPR 2018	1.6	13.5757	14.8
ContrastGAN [7]	ECCV 2018	8.3	14.8495	25.1
Pix2pix [2]	CVPR 2017	2.6	14.6118	-
Enc.-Decoder [2]	CVPR 2017	0.1	12.6660	-
BicycleGAN [43]	NIPS 2017	1.5	14.7914	-
AttentionGAN	Ours	12.8	14.9187	38.9

TABLE 3: AMT results of facial attribute transfer task on CelebA dataset. For this metric, higher is better.

Method	Publish	Hair Color	Gender	Aged
DIAT [37]	arXiv 2016	3.5	21.1	3.2
CycleGAN [3]	ICCV 2017	9.8	8.2	9.4
IcGAN [13]	NIPS 2016	1.3	6.3	5.7
StarGAN [14]	CVPR 2018	24.8	28.8	30.8
AttentionGAN	Ours	60.6	35.6	50.9

ablation studies. We gradually remove components of the proposed AttentionGAN, i.e., Attention-guided Discriminator (AD), Attention-guided Generator (AG), Attention Loss (AL) and Pixel Loss (PL). Results of AMT and PSNR on AR Face dataset are shown in Table 1. We find that removing one of them substantially degrades results, which means all of them are critical to our results. We also provide qualitative results in Fig. 4. Note that without AG we cannot generate both attention and content masks.

Attention-Guided Generation Scheme I vs. II Moreover, we present the comparison results of the proposed attention-guided generation schemes I and II. Schemes I is used in our conference paper [36]. Schemes II is a refined version proposed in this paper. Comparison results are shown in Fig. 5. We observe that scheme I generates good results on

TABLE 4: KID $\times 100 \pm \text{std.} \times 100$ of selfie to anime translation task. For this metric, lower is better.

Method	Publish	Selfie to Anime
U-GAT-IT [28]	ICLR 2020	11.61 \pm 0.57
CycleGAN [3]	ICCV 2017	13.08 \pm 0.49
UNIT [38]	NIPS 2017	14.71 \pm 0.59
MUNIT [39]	ECCV 2018	13.85 \pm 0.41
DRIT [40]	ECCV 2018	15.08 \pm 0.62
AttentionGAN	Ours	12.14 \pm 0.43

facial expression-to-expression translation task, however, it generates identical images with the inputs on other tasks, e.g., horse to zebra translation, apple to orange translation and map to aerial photo translation. The proposed attention-guided generation scheme II can handle all of these tasks.

4.2.2 Experiments on Face Images

We conduct facial expression translation experiments on four public datasets to validate the proposed AttentionGAN. These datasets contain faces with different races, styles and they have different illumination, occlusion, pose conditions and backgrounds.

Results on AR Face Dataset. Results of neutral \leftrightarrow happy translation on AR Face dataset are shown in Fig. 6. Clearly, the results of Dist.+Cycle and Self Dist. cannot even generate human faces. DiscoGAN produces identical results regardless of the input faces suffering from mode collapse. The results of DualGAN, DistanceGAN, StarGAN, Pix2pix, Encoder-Decoder and BicycleGAN tend to be blurry, while ComboGAN and ContrastGAN can produce the same identity but without expression changing. CycleGAN can generate sharper images, but the details of the generated faces are not convincing. Compared with all the baselines, the results of our AttentionGAN are more smooth, correct and with more details.

Results on CelebA Dataset. We conduct both facial expression translation and facial attribute transfer tasks on this dataset. Facial expression translation task on this dataset is more challenging than AR Face dataset since the background of this dataset is very complicated. Note that this

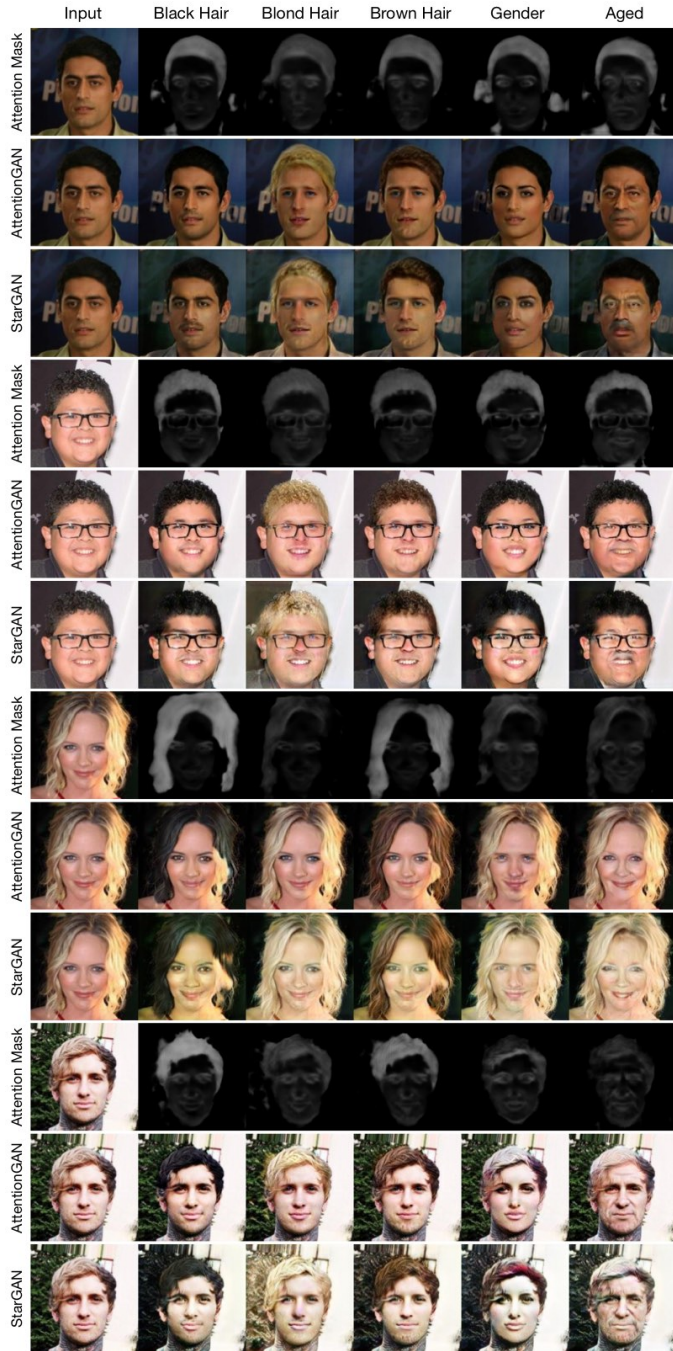


Fig. 8: Comparison with different methods on CelebA dataset for facial attribute transfer task.

dataset does not provide paired data, thus we cannot conduct experiments on supervised methods, i.e., Pix2pix, BicycleGAN and Encoder-Decoder. Results compared with other baselines are shown in Fig. 7. We observe that only the proposed AttentionGAN produces photo-realistic faces with correct expressions. The reason could be that methods without attention cannot learn the most discriminative part and the unwanted part. All existing methods failed to generate novel expressions, which means they treat the whole image as the unwanted part, while the proposed AttentionGAN can learn novel expressions, by distinguishing the discriminative part from the unwanted part.

Moreover, our model can be easily extended to solve

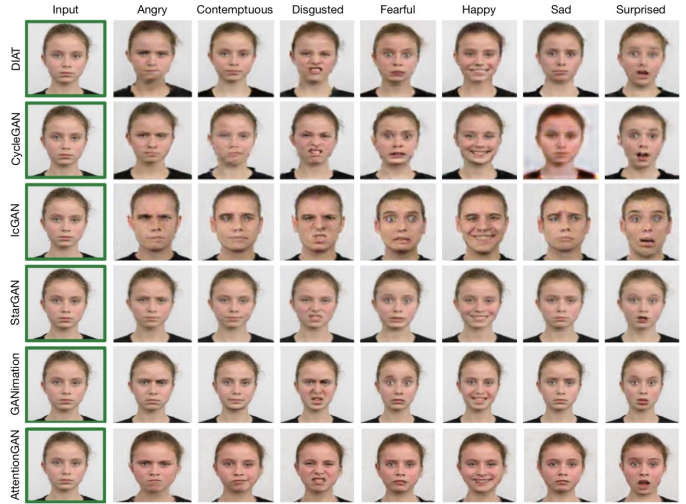


Fig. 9: Comparison with different methods on RaFD dataset.

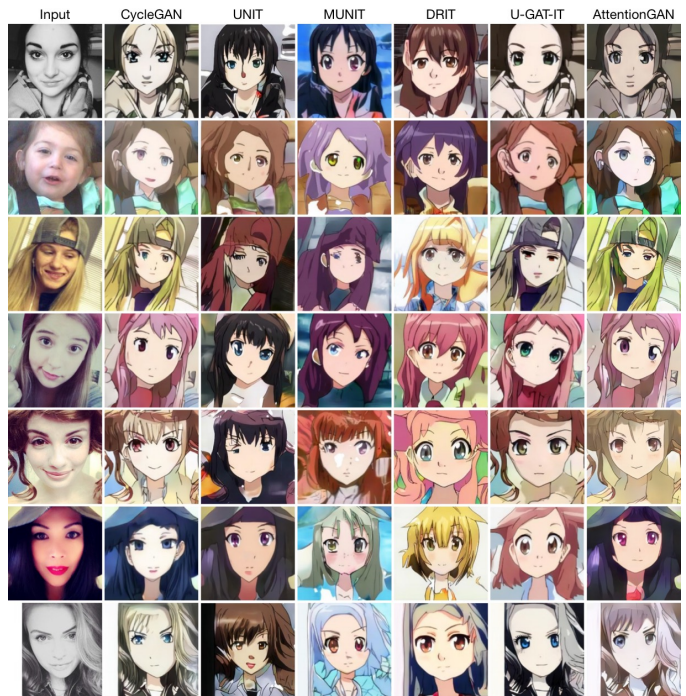


Fig. 10: Comparison with different methods for selfie to anime translation task.

multi-domain image-to-image translation problems. To control multiple domains in one single model we employ the domain classification loss proposed in StarGAN. Thus we follow StarGAN and conduct facial attribute transfer task on this dataset to evaluate the proposed AttentionGAN. Results compared with StarGAN are shown in Fig. 8. We observe that the proposed AttentionGAN achieves visually better results than StarGAN without changing backgrounds. **Results on RaFD Dataset.** We follow StarGAN and conduct diversity facial expression translation task on this dataset. Results compared against the baselines DIAT, CycleGAN, IcGAN, StarGAN and GANimation are shown in Fig. 9. We observe that the proposed AttentionGAN achieves better results than DIAT, CycleGAN, StarGAN and IcGAN. For GANimation, we follow the authors' instruction and use OpenFace [47] to obtain the action units of each face as extra input data. Note that the proposed method generate

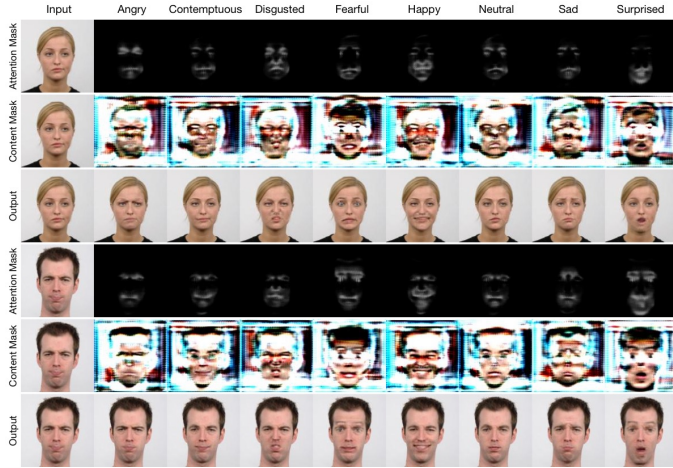


Fig. 11: Visualization of Learned attention and content masks on RaFD dataset.



Fig. 12: Visualization of Learned attention and content masks on CelebA dataset.

the competitive results compared to GANimation. However, GANimation needs action units annotations as extra training data, which limits its practical application. Moreover, GANimation cannot handle other generative tasks such facial attribute transfer as shown in Fig. 8.

Results of Selfie to Anime Translation. Following U-

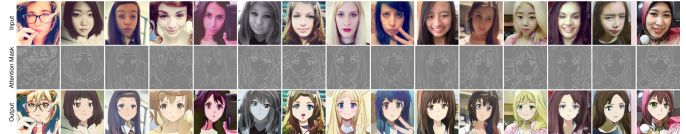


Fig. 13: Visualization of Learned attention on selfie to anime translation task.

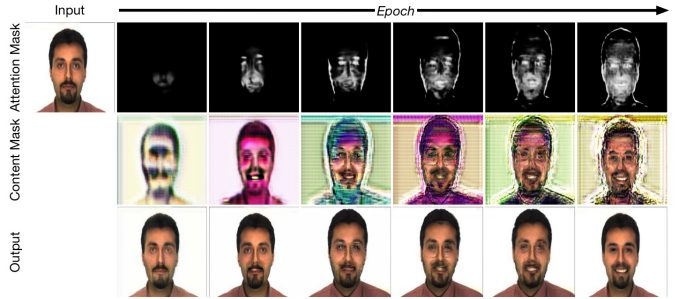


Fig. 14: Visualization of evolution of learned attention masks and content masks during training stage.

TABLE 5: Comparison of the overall model capacity on RaFD Dataset ($m=8$).

Method	Publish	# Models	# Parameters
Pix2pix [2]	CVPR 2017	m(m-1)	57.2M×56
Encoder-Decoder [2]	CVPR 2017	m(m-1)	41.9M×56
BicycleGAN [43]	NIPS 2017	m(m-1)	64.3M×56
CycleGAN [3]	ICCV 2017	m(m-1)/2	52.6M×28
DualGAN [4]	ICCV 2017	m(m-1)/2	178.7M×28
DiscoGAN [5]	ICML 2017	m(m-1)/2	16.6M×28
DistanceGAN [19]	NIPS 2017	m(m-1)/2	52.6M×28
Dist.+Cycle [19]	NIPS 2017	m(m-1)/2	52.6M×28
Self Dist. [19]	NIPS 2017	m(m-1)/2	52.6M×28
ComboGAN [20]	CVPR 2018	m	14.4M×8
StarGAN [14]	CVPR 2018	1	53.2M×1
ContrastGAN [7]	ECCV 2018	1	52.6M×1
AttentionGAN	Ours	1	52.6M×1

GAT-IT [28], we conduct selfie to anime translation on the Selfie2anime dataset. Results compared with state-of-the-art methods are shown in Fig. 10. We observe that the proposed AttentionGAN achieves better results than other methods.

We conclude that even though the subjects in these four datasets have different races, poses, styles, skin colors, illumination conditions, occlusions and complex backgrounds, our method consistently generates more sharper images with correct expressions/attributes than existing models. We also observe that our AttentionGAN preforms better than other baselines when training data are limited in Fig. 7, which also shows that our method is very robust.

Quantitative Comparison. We also provide quantitative results on these tasks. As shown in Table 2, we can see that the proposed AttentionGAN achieves the best results on these datasets compared with competing models including fully-supervised methods (e.g., Pix2pix, Encoder-Decoder and BicycleGAN) and mask-conditional methods (e.g., ContrastGAN). Next, following StarGAN, we perform a user study using Amazon Mechanical Turk (AMT) to assess attribute transfer task on CelebA dataset. Results compared the state-of-the-art methods are shown in Table 3. We observe that the proposed AttentionGAN achieves significantly better results than all the leading baselines. Moreover, following U-GAT-IT [28], we adopt KID to evaluate the generated images on selfie to anime translation. Results are shown in Table 4, we observe that our AttentionGAN achieves the

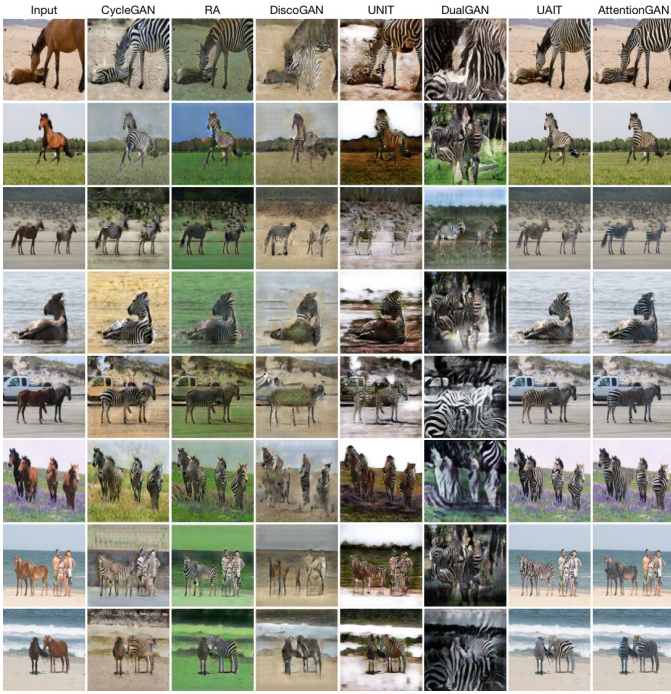


Fig. 15: Comparison with different methods on horse to zebra translation task.

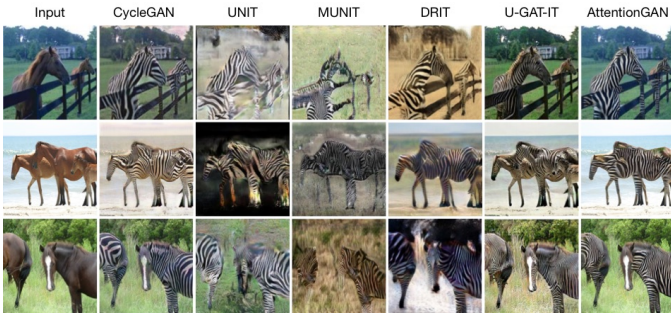


Fig. 16: Comparison with different methods on horse to zebra translation task.

best performance compared with all baselines except U-GAT-IT. However, U-GAT-IT needs to adopt two auxiliary classifiers to obtain attention maps, which significantly increases the number of network parameters and training time.

Visualization of Learned Attention and Content Masks.

Instead of regressing a full image, our generator outputs two masks, a content mask and an attention mask. We also visualize both masks on RaFD and CelebA datasets in Fig. 11 and Fig. 12, respectively. In Fig. 11, we observe that different expressions generate different attention masks and content masks. The proposed method makes the generator focus only on those discriminative regions of the image that are responsible of synthesizing the novel expression. The attention masks mainly focus on the eyes and mouth, which means these parts are important for generating novel expressions. The proposed method also keeps the other elements of the image or unwanted part untouched. In Fig. 11, the unwanted part are hair, cheek, clothes and also background, which means these parts have no contribution in generating novel expressions. In Fig. 12, we observe that different facial attributes also generate different attention

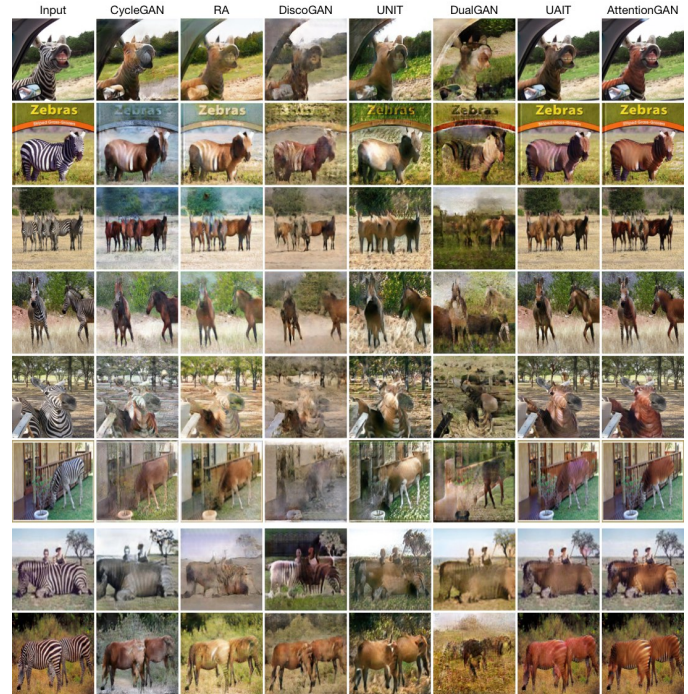


Fig. 17: Comparison with different methods on zebra to horse translation task.

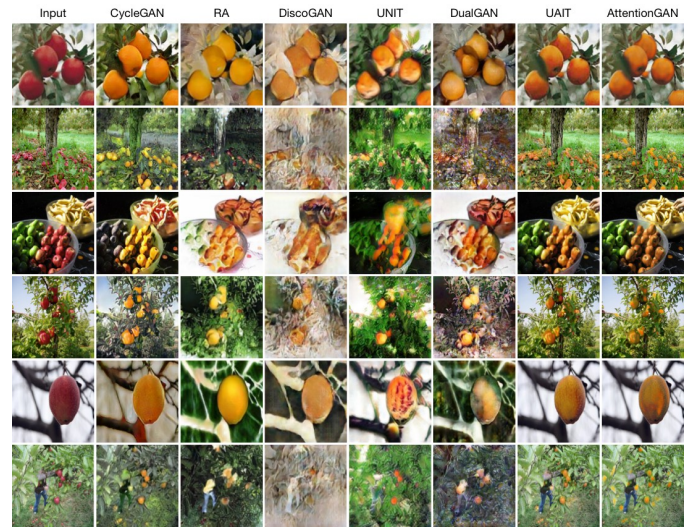


Fig. 18: Comparison with different methods on apple to orange translation task.

masks and content masks, which further validates our initial motivations. More attention masks generated by AttentionGAN on the facial attribute transfer task are shown in Fig. 8. Note that the proposed AttentionGAN can handle the geometric changes between source and target domains, such as selfie to anime translation. Therefore, we show the learned attention masks on selfie to anime translation task to interpret the generation process in Fig. 13.

We also present the generation of both masks on AR Face dataset epoch-by-epoch in Fig. 14. We see that with the number of training epoch increases, the attention mask and the result become better, and the attention masks correlate well with image quality, which demonstrates the proposed AttentionGAN is effective.

Comparison of the Number of Parameters. The number

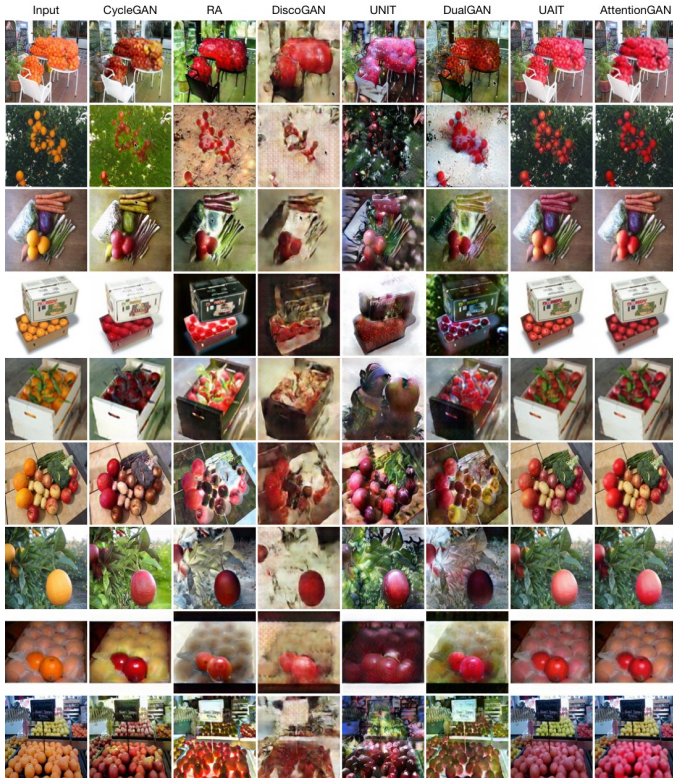


Fig. 19: Comparison with different methods on orange to apple translation task.

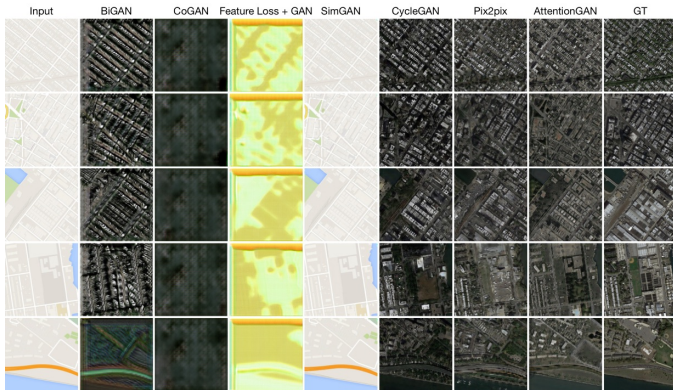


Fig. 20: Comparison with different methods on map to aerial photograph translation task.

of models for different m image domains and the number of model parameters on RaFD dataset are shown in Table 5. Note that our performance is much better than these baselines and the number of parameters is comparable with ContrastGAN, while ContrastGAN requires object masks as extra data.

4.2.3 Experiments on Natural Images

We conduct experiments on four natural image datasets to evaluate the proposed AttentionGAN.

Results of Horse ↔ Zebra Translation. Results of horse to zebra translation compared with CycleGAN, RA, DiscoGAN, UNIT, DualGAN and UAIT are shown in Fig. 15. We observe that DiscoGAN, UNIT, DualGAN generate blurred results. Both CycleGAN and RA can generate the corresponding zebras, however the background of images produced by both models has also been changed. Both UAIT

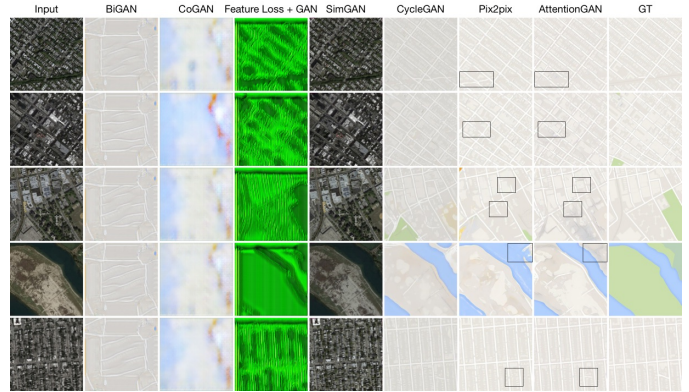


Fig. 21: Comparison with different methods on aerial photograph to map translation task.



Fig. 22: Comparison with different methods on style transfer task.

and the proposed AttentionGAN generate the corresponding zebras without changing the background. By carefully examining the translated images from both UAIT and the proposed AttentionGAN, we observe that AttentionGAN achieves slightly better results than UAIT as shown in the first and the second last rows of Fig. 15. Our method produces better stripes on the body of the lying horse than UAIT as shown in the first row. In the second last row, the proposed method generates fewer stripes on the body of the people than UAIT. Moreover, we compare the proposed method with CycleGAN, UNIT, MUNIT, DRIT and U-GAT-IT. Results are shown in Fig. 16. We can see that UNIT, MUNIT and DRIT generate blurred images with many visual artifacts. As observed in Fig. 15, CycleGAN can produce the corresponding zebras, however the background of images has also been changed. The just released U-GAT-IT and the proposed AttentionGAN can produce better results than other approaches. However, if we look closely at the results generated by both methods, we observe that U-GAT-IT slightly changes the background, while the proposed AttentionGAN perfectly keeps the background unchanged. For instance, as can be seen from the results of the first line, U-GAT-IT produces a darker background than the background of the input image in Fig. 16. However, the background color of the generated images by U-GAT-IT is lighter than the input images as shown in the second and third rows in Fig. 16. We also compare the proposed AttentionGAN with GANimorph and CycleGAN in Fig. 1. We see that the proposed AttentionGAN demonstrates a significant qualitative improvement over both methods.

Results of zebra to horse translation are shown in Fig. 17.



Fig. 23: Visualization of the learned attention masks on horse to zebra translation task.

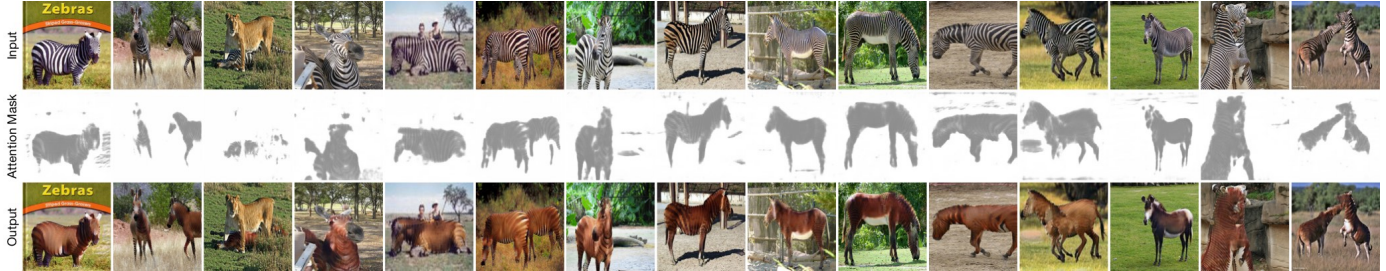


Fig. 24: Visualization of the learned attention masks on zebra to horse translation task.

TABLE 6: KID $\times 100 \pm \text{std.} \times 100$ for different methods. For this metric, lower is better. Abbreviations: (H)orse, (Z)ebra (A)pple, (O)range.

Method	Publish	H \rightarrow Z	Z \rightarrow H	A \rightarrow O	O \rightarrow A
DiscoGAN [5]	ICML 2017	13.68 \pm 0.28	16.60 \pm 0.50	18.34 \pm 0.75	21.56 \pm 0.80
RA [44]	CVPR 2017	10.16 \pm 0.12	10.97 \pm 0.26	12.75 \pm 0.49	13.84 \pm 0.78
DualGAN [4]	ICCV 2017	10.38 \pm 0.31	12.86 \pm 0.50	13.04 \pm 0.72	12.42 \pm 0.88
UNIT [38]	NIPS 2017	11.22 \pm 0.24	13.63 \pm 0.34	11.68 \pm 0.43	11.76 \pm 0.51
CycleGAN [3]	ICCV 2017	10.25 \pm 0.25	11.44 \pm 0.38	8.48 \pm 0.53	9.82 \pm 0.51
UAIT [29]	NeurIPS 2018	6.93 \pm 0.27	8.87 \pm 0.26	6.44 \pm 0.69	5.32 \pm 0.48
AttentionGAN	Ours	2.03 \pm 0.64	6.48 \pm 0.51	10.03 \pm 0.66	4.38 \pm 0.42

TABLE 7: Preference score of generated results on both horse to zebra and apple to orange translation tasks. For this metric, higher is better.

Method	Publish	Horse to Zebra	Apple to Orange
UNIT [38]	NIPS 2017	1.83	2.67
MUNIT [39]	ECCV 2018	3.86	6.23
DRIT [40]	ECCV 2018	1.27	1.09
CycleGAN [3]	ICCV 2017	22.12	26.76
U-GAT-IT [28]	ICLR 2020	33.17	30.05
AttentionGAN	Ours	37.75	33.20

We note that the proposed method generates better results than all the leading baselines. In summary, the proposed model is able to better alter the object of interest than existing methods by modeling attention masks in unpaired image-to-image translation tasks, without changing the background at the same time.

Results of Apple \leftrightarrow Orange Translation. Results compared with CycleGAN, RA, DiscoGAN, UNIT, DualGAN and UAIT are shown in Fig. 18 and 19. We observe that RA, DiscoGAN, UNIT and DualGAN generate blurred results with lots of visual artifacts. CycleGAN can generate better results, however, we can see that the background and other unwanted objects have also been changed. For example, the color of the banana in the third row of Fig. 18 has also been changed. Both UAIT and the proposed AttentionGAN can generate much better results than other baselines. However, UAIT adds an attention network before each generator to achieve the translation of the relevant parts, which increases the number of network parameters.

Results of Map \leftrightarrow Aerial Photo Translation. Qualitative results of both translation directions compared with existing methods are shown in Fig. 20 and 21, respectively. We note that BiGAN, CoGAN, SimGAN, Feature loss+GAN only generate blurred results with lots of visual artifacts. Results

TABLE 8: FID between generated samples and target samples for horse to zebra translation task. For this metric, lower is better.

Method	Publish	Horse to Zebra
UNIT [38]	NIPS 2017	241.13
CycleGAN [3]	ICCV 2017	109.36
SAT (Before Attention) [26]	TIP 2019	98.90
SAT (After Attention) [26]	TIP 2019	128.32
AttentionGAN	Ours	68.55

TABLE 9: AMT “real vs fake” results on maps \leftrightarrow aerial photos. For this metric, higher is better.

Method	Publish	Map to Photo	Photo to Map
CoGAN [41]	NIPS 2016	0.8 \pm 0.7	1.3 \pm 0.8
BiGAN/ALI [45], [46]	ICLR 2017	3.2 \pm 1.5	2.9 \pm 1.2
SimGAN [42]	CVPR 2017	0.4 \pm 0.3	2.2 \pm 0.7
Feature loss + GAN [42]	CVPR 2017	1.1 \pm 0.8	0.5 \pm 0.3
CycleGAN [3]	ICCV 2017	27.9 \pm 3.2	25.1 \pm 2.9
Pix2pix [2]	CVPR 2017	33.7 \pm 2.6	29.4 \pm 3.2
AttentionGAN	Ours	35.18 \pm 2.9	32.4 \pm 2.5

generated by our method are better than those generated by CycleGAN. Moreover, we compare the proposed method with the fully supervised Pix2pix, we see that the proposed method achieves comparable or even better results than Pix2pix as indicated in the black boxes in Fig. 21.

Results of Style Transfer. Lastly, we also show the generation results of the proposed AttentionGAN on the style transfer task. Results compared with the leading method, i.e., CycleGAN, are shown in Fig. 22. We observe that the proposed AttentionGAN generates much sharper and diverse results than CycleGAN.

Quantitative Comparison. We follow UAIT [29] and adopt Kernel Inception Distance (KID) [48] to evaluate the generated images by different methods. Results compared with different baselines on both horse \leftrightarrow zebra translation and apple \leftrightarrow orange translation tasks are shown in Table 6. We observe that our AttentionGAN achieves the lowest KID on H \rightarrow Z, Z \rightarrow H and O \rightarrow A translation tasks. We note that both UAIT and CycleGAN produce a lower KID score on apple to orange translation (A \rightarrow O) but have poor quality image generation as shown in Fig. 18.

Moreover, following U-GAT-IT [28], we conduct a perceptual study to evaluate the generated images. Specifically, 50 participants are shown the generated images from different methods including our AttentionGAN with source



Fig. 25: Visualization of the learned attention masks on apple to orange translation task.

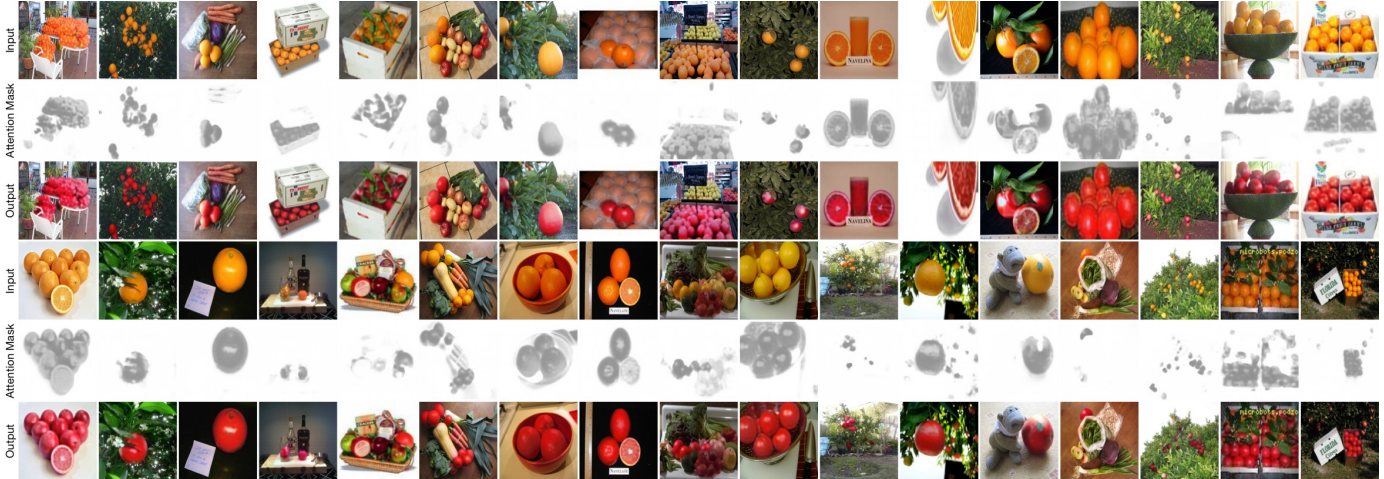


Fig. 26: Visualization of the learned attention masks on orange to apple translation task.



Fig. 27: Visualization of the learned attention masks compared with SAT [26] on horse to zebra translation task. Most significantly improved regions are highlighted with red boxes.

image, and asked to select the best generated image to target

domain, i.e., zebra and orange. Note that this evaluation protocol of user study is different from the one used in CycleGAN. Results of both horse to zebra translation and apple to orange translation are shown in Table 7. We observe that the proposed method outperforms other baselines including U-GAT-IT on both tasks.

Next, we follow SAT [26] and adopt Fréchet Inception Distance (FID) [49] to measure the distance between generated samples and target samples. We compute FID for horse to zebra translation and results compared with SAT, CycleGAN and UNIT are shown in Table 8. We observe that the proposed model achieves significantly better FID than all baselines. We note that SAT with attention has worse FID than SAT without attention, which means using attention might have a negative effect on FID because there might be some correlations between foreground and background in the target domain when computing FID. While we did not observe such negative effect on the proposed AttentionGAN. Qualitative comparison with SAT is shown in Fig. 27. We observe that the proposed AttentionGAN achieves better results than SAT.

Finally, we follow CycleGAN and adopt AMT score to evaluate the generated images on the map \leftrightarrow aerial photo translation task. Participants were shown a sequence of pairs of images, one real photo or map and one fake generated by our method or existing methods, and asked to click on the image they thought was real. Comparison results of both translation directions are shown in Table 9. We observe that the proposed AttentionGAN generate the

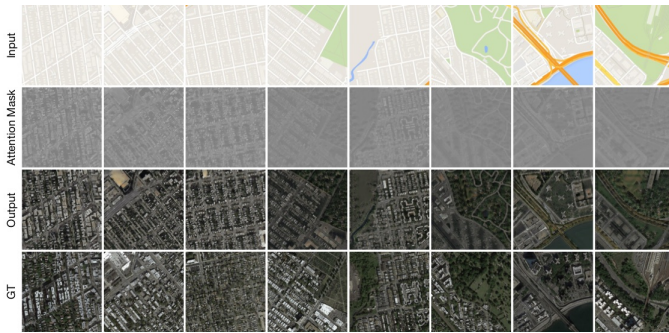


Fig. 28: Visualization of the learned attention masks on map to aerial photo translation.

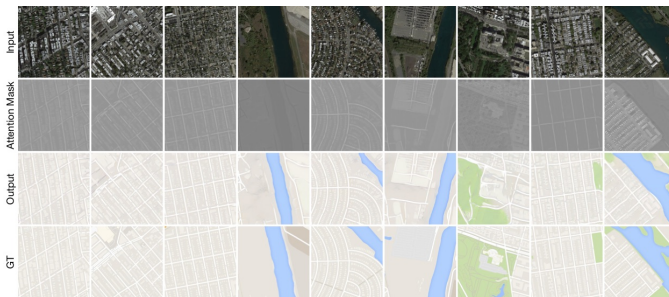


Fig. 29: Visualization of the learned attention masks on aerial photo to map translation.

best results compared with the leading methods and can fool participants on around 1/3 of trials in both translation directions.

Visualization of Learned Attention Masks. We show the learned attention masks on these tasks. Results of both horse \leftrightarrow zebra translation and apple \leftrightarrow orange translation tasks are shown in Fig. 23, 24, 25 and 26, respectively. We observe that the proposed AttentionGAN is able to learn relevant image regions and ignore the background and other irrelevant objects. Moreover, we also compare with the most recently method, SAT [26], on the learned attention masks. Results are shown in Fig. 27. We observe that the attention masks learned by our method are much accurate than those generated by SAT, especially in the boundary of attended objects. Thus our method generates more photo-realistic object boundary than SAT in the translated images, as indicated in the red boxes in Fig. 27.

Moreover, we also show some examples of the learned attention masks on the map \leftrightarrow aerial photo translation task. Results are shown in Fig. 28 and 29, respectively. Note that although images of the source and target domains differ greatly on the appearance, the images of both domains are structurally identical. Thus the learned attention masks highlight the shared layout and structure of both source and target domains. Thus we can conclude that the proposed AttentionGAN can handle both images requiring large shape changes and images requiring holistic changes.

5 CONCLUSION

We propose a novel attention-guided GAN model, i.e., AttentionGAN, for both unpaired image-to-image translation and multi-domain image-to-image translation tasks. The generators in AttentionGAN have the built-in attention mechanism, which can preserve the background of the input

images and discover the most discriminative content between the source and target domains by producing attention masks and content masks. Then the attention masks, content masks and the input images are combined to generate the target images with high-quality. Extensive experimental results on several challenging tasks demonstrate that the proposed AttentionGAN can generate better results with more convincing details than numerous state-of-the-art methods.

ACKNOWLEDGEMENTS

This work is partially supported by National Natural Science Foundation of China (NSFC, No.U1613209,61673030), Shenzhen Key Laboratory for Intelligent Multimedia and Virtual Reality (ZDSYS201703031405467).

REFERENCES

- [1] I. Goodfellow, J. Pouget-Abadie, M. Mirza, B. Xu, D. Warde-Farley, S. Ozair, A. Courville, and Y. Bengio, "Generative adversarial nets," in *NIPS*, 2014. 1, 3, 6
- [2] P. Isola, J.-Y. Zhu, T. Zhou, and A. A. Efros, "Image-to-image translation with conditional adversarial networks," in *CVPR*, 2017. 1, 3, 6, 7, 8, 10, 13
- [3] J.-Y. Zhu, T. Park, P. Isola, and A. A. Efros, "Unpaired image-to-image translation using cycle-consistent adversarial networks," in *ICCV*, 2017. 1, 2, 3, 4, 5, 6, 7, 8, 10, 13
- [4] Z. Yi, H. Zhang, P. Tan, and M. Gong, "Dualgan: Unsupervised dual learning for image-to-image translation," in *ICCV*, 2017. 1, 3, 4, 7, 8, 10, 13
- [5] T. Kim, M. Cha, H. Kim, J. Lee, and J. Kim, "Learning to discover cross-domain relations with generative adversarial networks," in *ICML*, 2017. 1, 3, 7, 8, 10, 13
- [6] A. Gokaslan, V. Ramanujan, D. Ritchie, K. In Kim, and J. Tompkin, "Improving shape deformation in unsupervised image-to-image translation," in *ECCV*, 2018. 1, 2, 7
- [7] X. Liang, H. Zhang, and E. P. Xing, "Generative semantic manipulation with contrasting gan," in *ECCV*, 2018. 1, 3, 7, 8, 10
- [8] X. Chen, C. Xu, X. Yang, and D. Tao, "Attention-gan for object transfiguration in wild images," in *ECCV*, 2018. 1, 3
- [9] D. Kastaniotis, I. Ntinou, D. Tsourounis, G. Economou, and S. Fotopoulos, "Attention-aware generative adversarial networks (atagans)," in *IVMSP Workshop*, 2018. 1, 3
- [10] A. Brock, J. Donahue, and K. Simonyan, "Large scale gan training for high fidelity natural image synthesis," in *ICLR*, 2019. 3
- [11] Y. Wang, C. Wu, L. Herranz, J. van de Weijer, A. Gonzalez-Garcia, and B. Raducanu, "Transferring gans: generating images from limited data," in *ECCV*, 2018. 3
- [12] M. Mirza and S. Osindero, "Conditional generative adversarial nets," *arXiv preprint arXiv:1411.1784*, 2014. 3
- [13] G. Perarnau, J. van de Weijer, B. Raducanu, and J. M. Álvarez, "Invertible conditional gans for image editing," in *NIPS Workshop*, 2016. 3, 7, 8
- [14] Y. Choi, M. Choi, M. Kim, J.-W. Ha, S. Kim, and J. Choo, "Stargan: Unified generative adversarial networks for multi-domain image-to-image translation," in *CVPR*, 2018. 3, 6, 7, 8, 10
- [15] S. E. Reed, Z. Akata, S. Mohan, S. Tenka, B. Schiele, and H. Lee, "Learning what and where to draw," in *NIPS*, 2016. 3
- [16] H. Tang, W. Wang, D. Xu, Y. Yan, and N. Sebe, "Gesturegan for hand gesture-to-gesture translation in the wild," in *ACM MM*, 2018. 3
- [17] T.-C. Wang, M.-Y. Liu, J.-Y. Zhu, A. Tao, J. Kautz, and B. Catanzaro, "High-resolution image synthesis and semantic manipulation with conditional gans," in *CVPR*, 2018. 3
- [18] H. Tang, D. Xu, N. Sebe, Y. Wang, J. J. Corso, and Y. Yan, "Multi-channel attention selection gan with cascaded semantic guidance for cross-view image translation," in *CVPR*, 2019. 3
- [19] S. Benaim and L. Wolf, "One-sided unsupervised domain mapping," in *NIPS*, 2017. 3, 7, 8, 10
- [20] A. Anosheh, E. Agustsson, R. Timofte, and L. Van Gool, "Combogan: Unrestrained scalability for image domain translation," in *CVPR Workshop*, 2018. 3, 7, 8, 10

- [21] H. Tang, D. Xu, W. Wang, Y. Yan, and N. Sebe, "Dual generator generative adversarial networks for multi-domain image-to-image translation," in *ACCV*, 2018. 3
- [22] Y. Wang, J. van de Weijer, and L. Herranz, "Mix and match networks: encoder-decoder alignment for zero-pair image translation," in *CVPR*, 2018. 3
- [23] D. Xu, W. Wang, H. Tang, H. Liu, N. Sebe, and E. Ricci, "Structured attention guided convolutional neural fields for monocular depth estimation," in *CVPR*, 2018. 3
- [24] R. Sun, C. Huang, J. Shi, and L. Ma, "Mask-aware photorealistic face attribute manipulation," *arXiv preprint arXiv:1804.08882*, 2018. 3
- [25] S. Mo, M. Cho, and J. Shin, "Instagan: Instance-aware image-to-image translation," in *ICLR*, 2019. 3
- [26] C. Yang, T. Kim, R. Wang, H. Peng, and C.-C. J. Kuo, "Show, attend and translate: Unsupervised image translation with self-regularization and attention," *IEEE TIP*, 2019. 3, 7, 13, 14, 15
- [27] H. Zhang, I. Goodfellow, D. Metaxas, and A. Odena, "Self-attention generative adversarial networks," in *ICML*, 2019. 3
- [28] J. Kim, M. Kim, H. Kang, and K. Lee, "U-gat-it: Unsupervised generative attentional networks with adaptive layer-instance normalization for image-to-image translation," 2020. 3, 7, 8, 10, 13
- [29] Y. A. Mejjati, C. Richardt, J. Tompkin, D. Cosker, and K. I. Kim, "Unsupervised attention-guided image to image translation," in *NeurIPS*, 2018. 3, 7, 13
- [30] A. Pumarola, A. Agudo, A. M. Martinez, A. Sanfeliu, and F. Moreno-Noguer, "Ganimation: Anatomically-aware facial animation from a single image," in *ECCV*, 2018. 6, 7
- [31] X. Mao, Q. Li, H. Xie, R. Y. Lau, and Z. Wang, "Multi-class generative adversarial networks with the l2 loss function," *arXiv preprint arXiv:1611.04076*, 2016. 6
- [32] Z. Liu, P. Luo, X. Wang, and X. Tang, "Deep learning face attributes in the wild," in *ICCV*, 2015. 6
- [33] O. Langner, R. Dotsch, G. Bijlstra, D. H. Wigboldus, S. T. Hawk, and A. Van Knippenberg, "Presentation and validation of the radboud faces database," *Cognition and Emotion*, vol. 24, no. 8, pp. 1377–1388, 2010. 7
- [34] A. M. Martinez, "The ar face database," *CVC TR*, 1998. 7
- [35] D. Kingma and J. Ba, "Adam: A method for stochastic optimization," in *ICLR*, 2014. 7
- [36] H. Tang, D. Xu, N. Sebe, and Y. Yan, "Attention-guided generative adversarial networks for unsupervised image-to-image translation," in *IJCNN*, 2019. 7, 8
- [37] M. Li, W. Zuo, and D. Zhang, "Deep identity-aware transfer of facial attributes," *arXiv preprint arXiv:1610.05586*, 2016. 7, 8
- [38] M.-Y. Liu, T. Breuel, and J. Kautz, "Unsupervised image-to-image translation networks," in *NIPS*, 2017. 7, 8, 13
- [39] X. Huang, M.-Y. Liu, S. Belongie, and J. Kautz, "Multimodal unsupervised image-to-image translation," in *ECCV*, 2018. 7, 8, 13
- [40] H.-Y. Lee, H.-Y. Tseng, J.-B. Huang, M. Singh, and M.-H. Yang, "Diverse image-to-image translation via disentangled representations," in *ECCV*, 2018. 7, 8, 13
- [41] M.-Y. Liu and O. Tuzel, "Coupled generative adversarial networks," in *NIPS*, 2016. 7, 13
- [42] A. Shrivastava, T. Pfister, O. Tuzel, J. Susskind, W. Wang, and R. Webb, "Learning from simulated and unsupervised images through adversarial training," in *CVPR*, 2017. 7, 13
- [43] J.-Y. Zhu, R. Zhang, D. Pathak, T. Darrell, A. A. Efros, O. Wang, and E. Shechtman, "Toward multimodal image-to-image translation," in *NIPS*, 2017. 7, 8, 10
- [44] F. Wang, M. Jiang, C. Qian, S. Yang, C. Li, H. Zhang, X. Wang, and X. Tang, "Residual attention network for image classification," in *CVPR*, 2017. 7, 13
- [45] J. Donahue, P. Krähenbühl, and T. Darrell, "Adversarial feature learning," in *ICLR*, 2017. 7, 13
- [46] V. Dumoulin, I. Belghazi, B. Poole, O. Mastropietro, A. Lamb, M. Arjovsky, and A. Courville, "Adversarially learned inference," in *ICLR*, 2017. 7, 13
- [47] T. Baltrušaitis, P. Robinson, and L.-P. Morency, "Openface: an open source facial behavior analysis toolkit," in *WACV*, 2016. 7, 9
- [48] M. Bińkowski, D. J. Sutherland, M. Arbel, and A. Gretton, "Demystifying mmd gans," in *ICLR*, 2018. 7, 13
- [49] M. Heusel, H. Ramsauer, T. Unterthiner, B. Nessler, and S. Hochreiter, "Gans trained by a two time-scale update rule converge to a local nash equilibrium," in *NIPS*, 2017. 7, 14



Hao Tang is a Ph.D. candidate in the Department of Information Engineering and Computer Science, and a member of Multimedia and Human Understanding Group (MHUG) led by Prof. Nicu Sebe at the University of Trento. He received the Master degree in computer application technology in 2016 at the School of Electronics and Computer Engineering, Peking University, China. His research interests are machine learning, human-computer interaction, (deep) representation learning, robotics and their applications to computer vision.



Hong Liu received the Ph.D. degree in mechanical electronics and automation in 1996, and serves as a Full Professor in the School of EE&CS, Peking University (PKU), China. Prof. Liu has been selected as Chinese Innovation Leading Talent supported by National High-level Talents Special Support Plan since 2013. He is also the Director of Open Lab on Human Robot Interaction, PKU, his research fields include computer vision and robotics, image processing, and pattern recognition. He is an IEEE

member, vice president of Chinese Association for Artificial Intelligence (CAAI), and vice chair of Intelligent Robotics Society of CAAI.



Dan Xu is a Postdoc researcher in Visual Geometric Group at the University of Oxford. He received the Ph.D. Computer Science at the University of Trento. He was a research assistant in the Multimedia Laboratory in the Department of Electronic Engineering at the Chinese University of Hong Kong. His research focuses on computer vision, multimedia and machine learning. Specifically, he is interested in deep learning, structured prediction and cross-modal representation learning and the applications to 2D/3D

scene understanding tasks. He received the Intel best scientific paper award at ICPR 2016.



Philip H. S. Torr received the PhD degree from Oxford University. After working for another three years at Oxford, he worked for six years for Microsoft Research, first in Redmond, then in Cambridge, founding the vision side of the Machine Learning and Perception Group. He is now a professor at Oxford University. He has won awards from top vision conferences, including ICCV, CVPR, ECCV, NIPS and BMVC. He is a senior member of the IEEE and a Royal Society Wolfson Research Merit Award holder.



Nicu Sebe is Professor with the University of Trento, Italy, leading the research in the areas of multimedia information retrieval and human behavior understanding. He was the General CoChair of the IEEE FG Conference 2008 and ACM Multimedia 2013, and the Program Chair of the International Conference on Image and Video Retrieval in 2007 and 2010, ACM Multimedia 2007 and 2011. He is the Program Chair of ICCV 2017 and ECCV 2016, and a General Chair of ACM ICMR 2017 and ICPR 2020. He is

a fellow of the International Association for Pattern Recognition.